

Electronic Supplementary Information

***In situ* fabrication of luminescent copper nanoclusters/eggshell
membrane composite and applications for visual detection of Ag⁺
ions, light-emitting diodes and surface patterning**

Chunbo Li, Congying Shao,* Lu Li, Xianhu Liu and Mingzhu Liu

College of Chemistry and Materials Science, Huaibei Normal University,

Huaibei, Anhui 235000, China

Email: shaocongying@163.com

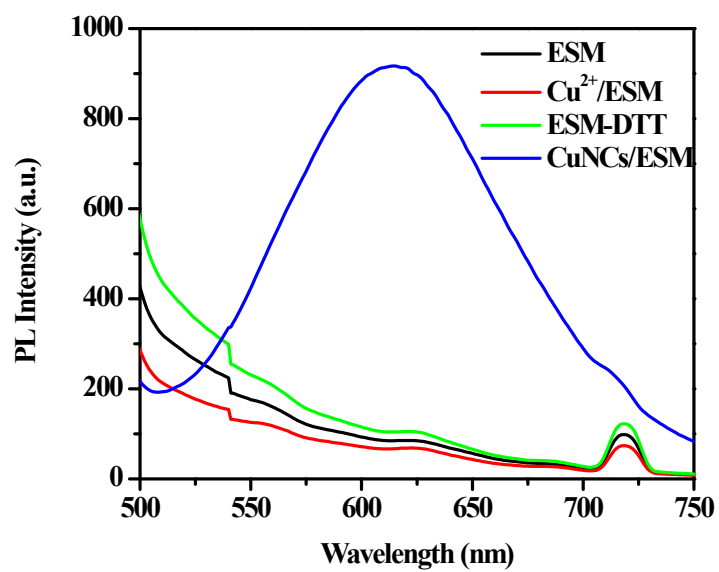


Fig. S1. PL emission spectra of ESM, Cu²⁺/ESM, ESM-DTT and Cu NCs/ESM excited by 365 nm.

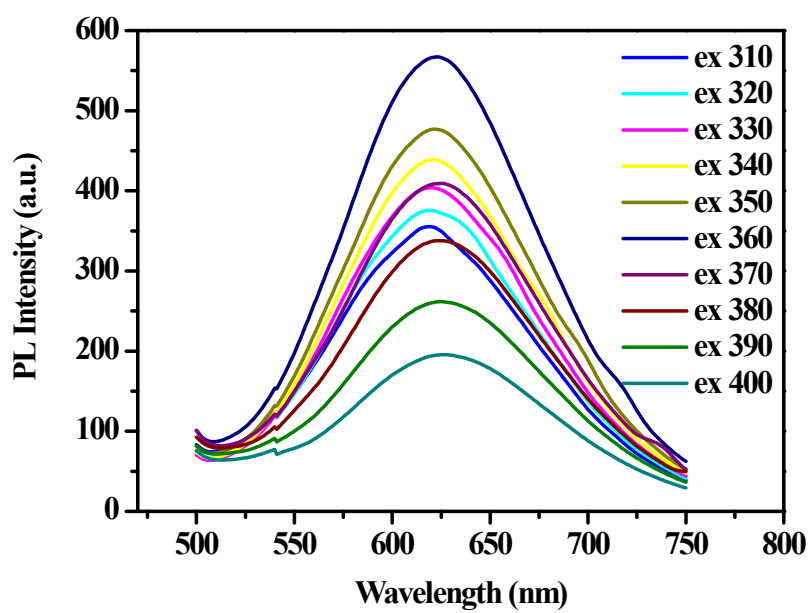


Fig. S2. PL spectra of wet Cu NCs/ESM varying excitation wavelengths from 310 to 400 nm.

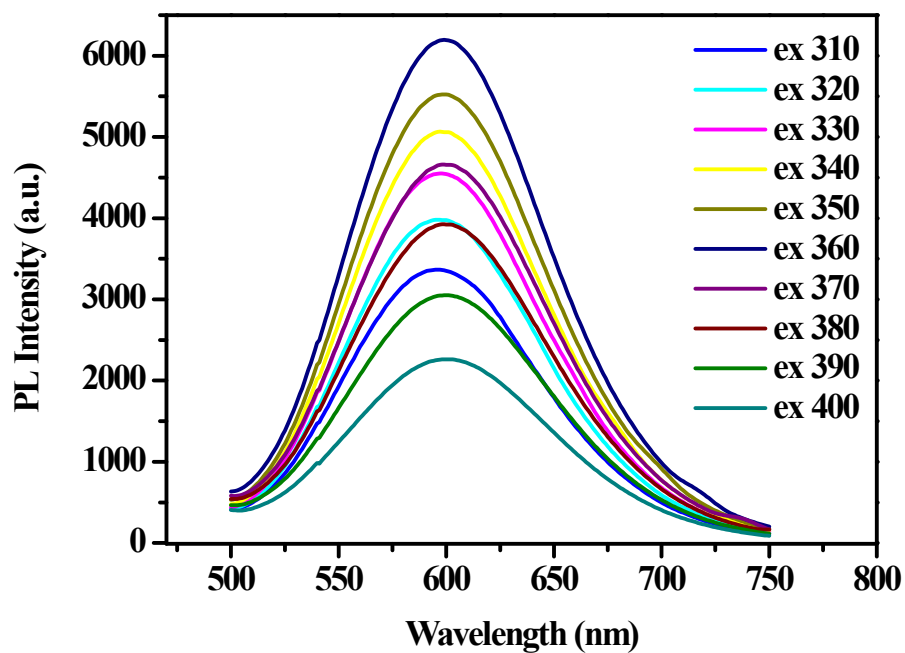
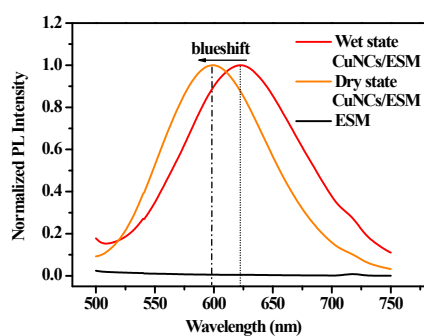


Fig. S3. PL spectra of dried Cu NCs/ESM varying excitation wavelengths from 310 to 400 nm.

(a)



(b)

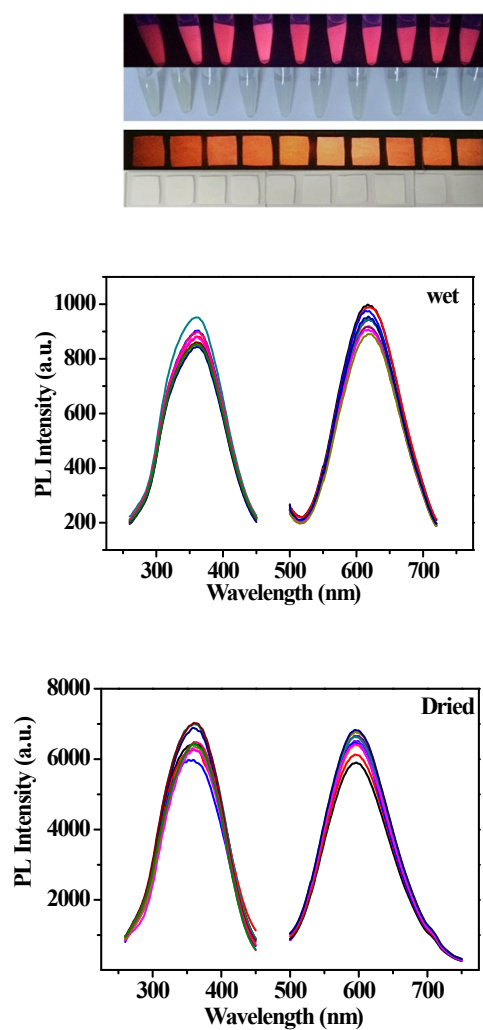
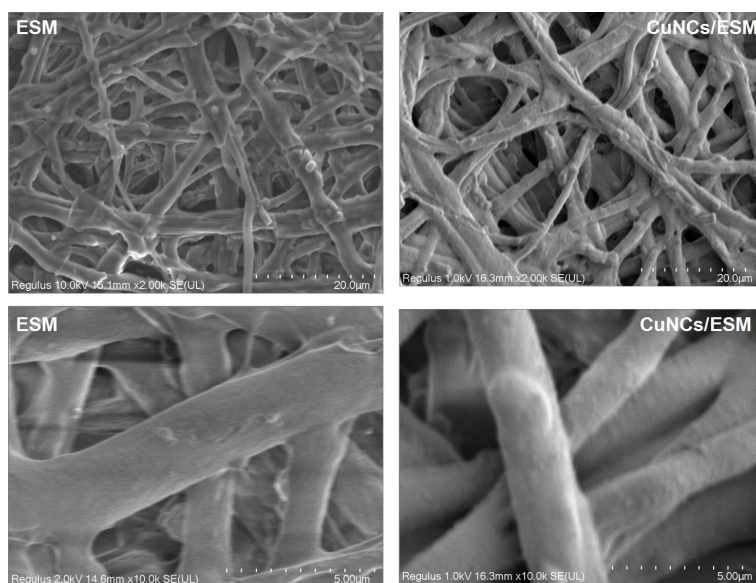


Fig. S4. (a) Comparison of normalized emission spectra of wet and dried Cu NCs/ESM composites indicating blue shift during the natural dehydration process. (b) Photos and excitation/emission spectra of ten wet and dried Cu NCs/ESM products fabricated at the same conditions, indicating the simplicity and good reproducibility of the fabrication.

(a)



(b)

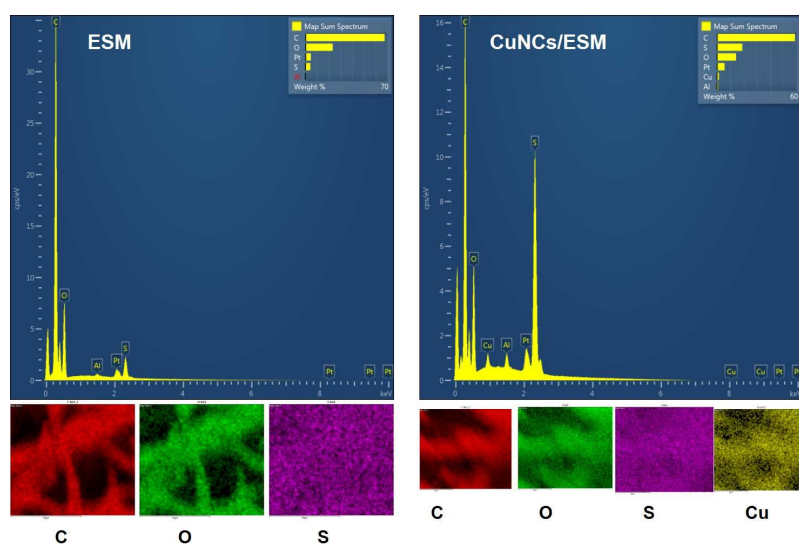


Fig. S5. (a) SEM images of ESM matrix and fabricated Cu NCs/ESM nanocomposite at different magnification. (b) Energy spectra and element mapping results of C, O, N, S and Cu of ESM and Cu NCs/ESM, respectively.

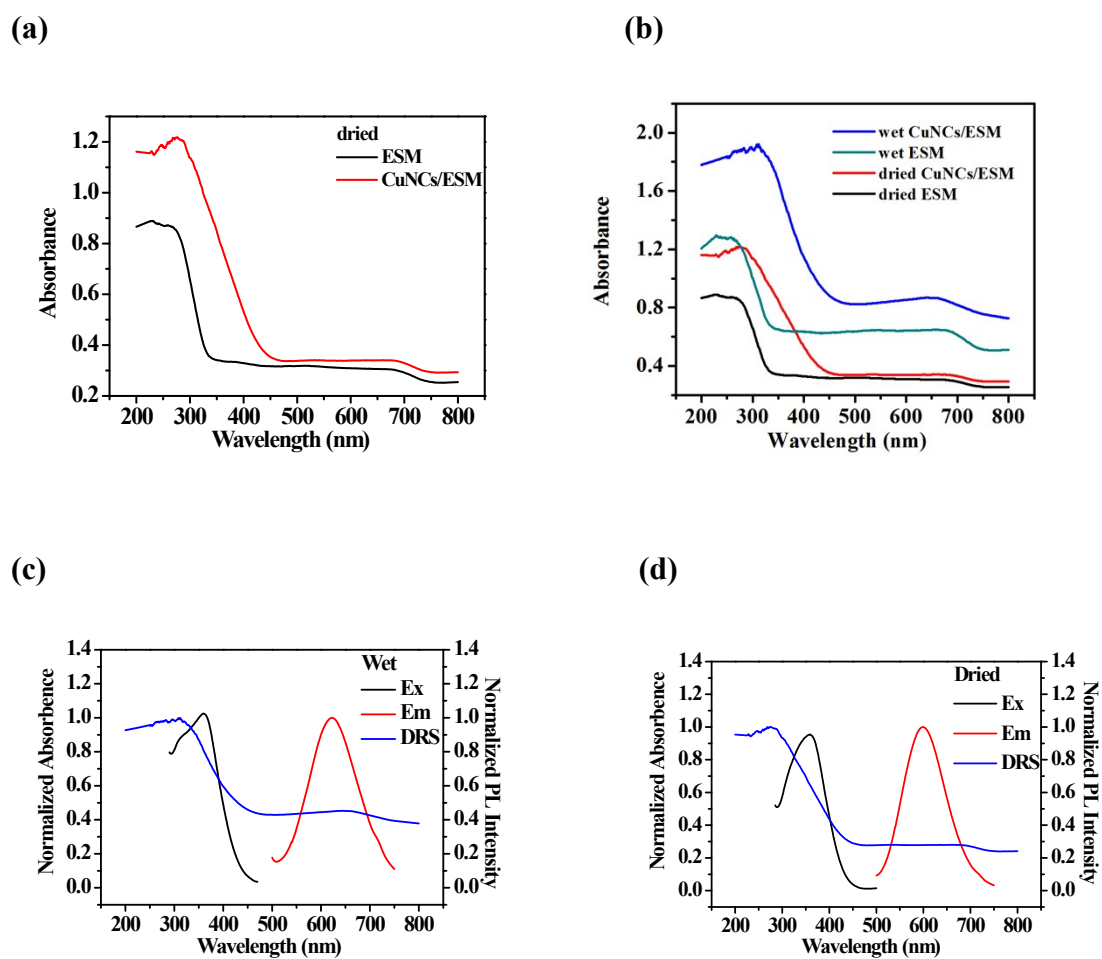


Fig. S6. (a) The UV-vis DRS spectra of dried Cu NCs/ESM composite and ESM matrix, respectively. (b) The comparison of DRS spectra of wet and dried Cu NCs/ESM composites and their ESMs. The superimposition of DRS spectra and their PL spectra of wet (c) and dried (d) Cu NCs/ESM composites, respectively.

(a)

τ_1 (ns)	τ_2 (ns)	τ_3 (ns)	A_1	A_2	A_3	Rel ₁ %	Rel ₂ %	Rel ₃ %	τ_{average} (ns)	χ^2
324.103	2233.82	10185	15923.8	211.723	78.7077	80.2	7.35	12.45	1692.76	1.108

(b)

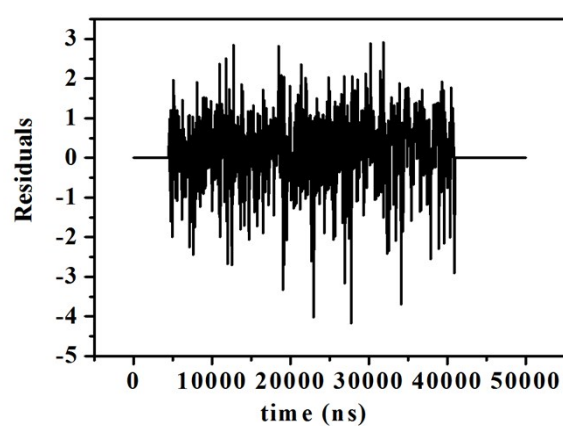


Fig. S7. (a) The data derived from fitting the decay curve of fabricated Cu NCs/ESM by three exponential function. The average PL lifetime of generated Cu NCs was calculated based on the equation: $\tau_{\text{average}} = (A_1\tau_1^2 + A_2\tau_2^2 + A_3\tau_3^2) / (A_1\tau_1 + A_2\tau_2 + A_3\tau_3)$. The Rel% of each lifetime component was calculated based on the equation: $\text{Rel}_i\% = A_i\tau_i / (A_1\tau_1 + A_2\tau_2 + A_3\tau_3) \times 100$. (b) The residuals curve of the fitting process.

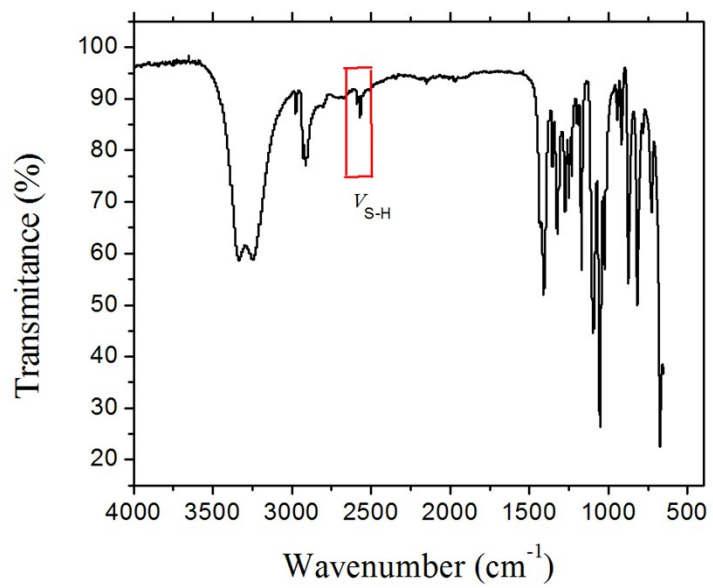
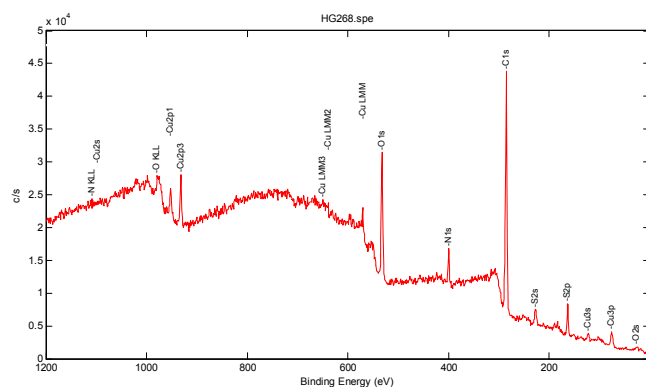
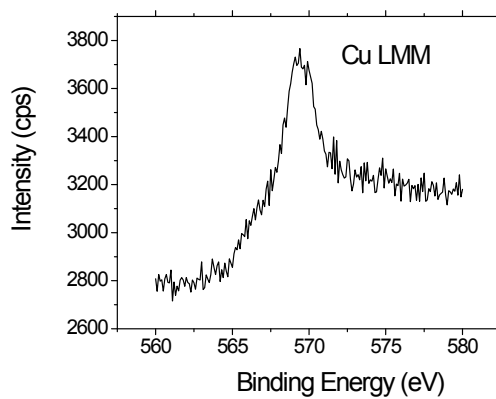


Fig. S8. The FTIR spectrum of pure DTT agent.

(a)



(b)



(c)

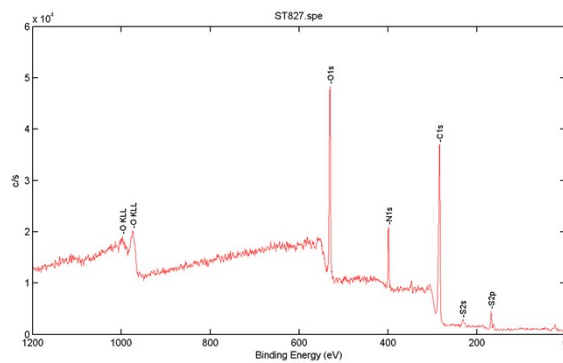


Fig. S9. The XPS survey spectra of fabricated Cu NCs/ESM composite (a) and ESM matrix (c). (b) The Auger electron spectrum (AES) in the Cu LMM region of Cu NCs/ESM. The AES Cu (LMM) peak at 569.5 eV indicated the exact presence of Cu(I) component in the Cu NCs.

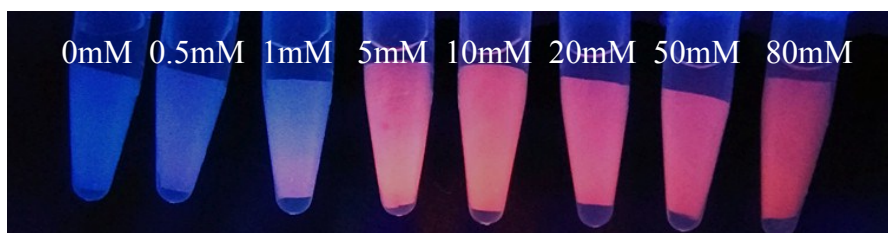


Fig. S10. The influence of CuSO_4 concentration on the luminescence of resultant Cu NCs/ESM composite. ESMs were pre-incubated in CuSO_4 solutions with different concentrations: 0, 0.5, 1, 5, 10, 20, 50 and 80 mM (from left to right) for 15 min, and then transferred to 0.5 M DTT solution to initialize the reduction process. The photo of the samples was taken under 365 nm UV light after a reaction time of 1.5 h at room temperature.

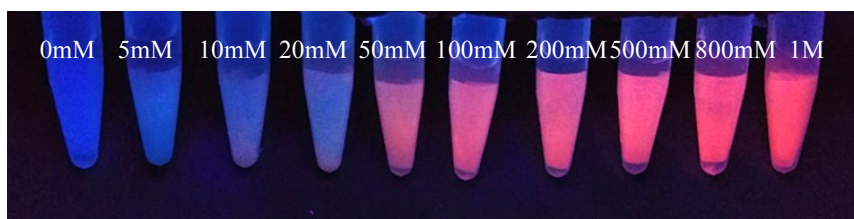


Fig. S11. The influence of DTT concentration on the luminescence of resultant Cu NCs/ESM composite. ESMs were pre-incubated in CuSO_4 solutions (1 mL, 50 mM) for 15min, and then transferred to DTT solutions with various concentrations: 0, 0.005, 0.01, 0.02, 0.05, 0.1, 0.2, 0.5, 0.8, 1 M (from left to right) to initialize the reduction process. The photo of the samples was taken under 365 nm UV light after a reaction time of 1.5 h at room temperature.

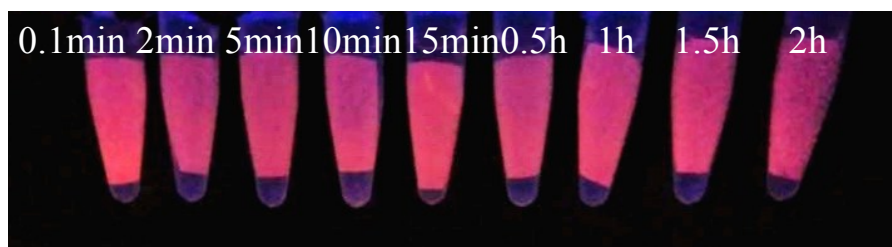


Fig.S12. The influence of incubation time of the ESM with CuSO_4 precursor on the luminescence of resultant Cu NCs/ESM composite. ESMs were incubated with CuSO_4 solution (1 mL, 50 mM) for different time (0.1, 2, 5, 10, 15, 30, 60, 90, 120 min, from left to right tubes), and finally transferred to DTT solution (1 mL, 0.5 M). The luminescence image of the samples was taken under 365 nm UV light after a reaction time of 1.5 h at room temperature.

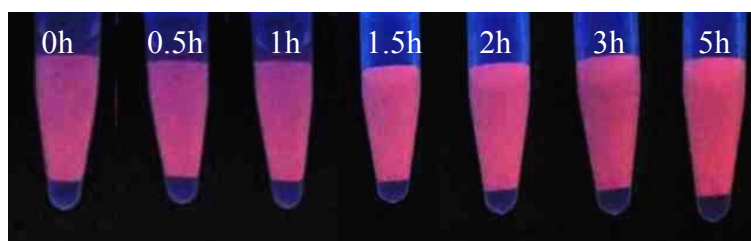


Fig. S13. Luminescence evolution of the Cu^{2+} /ESM complex with DTT solution for different reaction time. ESM was incubated in CuSO_4 solution (1 mL, 50 mM) for 15 min, and then transferred to DTT solution (1 mL, 0.5 M) for different reaction time (0, 0.5, 1, 1.5, 2, 3, 5 h, from left to right). The photos of the samples were taken under 365 nm UV light at different reaction time .



Fig. S14. The effect of different copper precursors on the fabrication of luminescent Cu NCs/ESM composite. Various copper precursors (CuSO_4 , $\text{Cu}(\text{CH}_3\text{COO})_2$, $\text{Cu}(\text{NO}_3)_2$, CuCl_2) were employed in the fabrication (from left to right tubes). Photos of the samples were taken under room light (left) and 365 nm UV light (right), respectively.

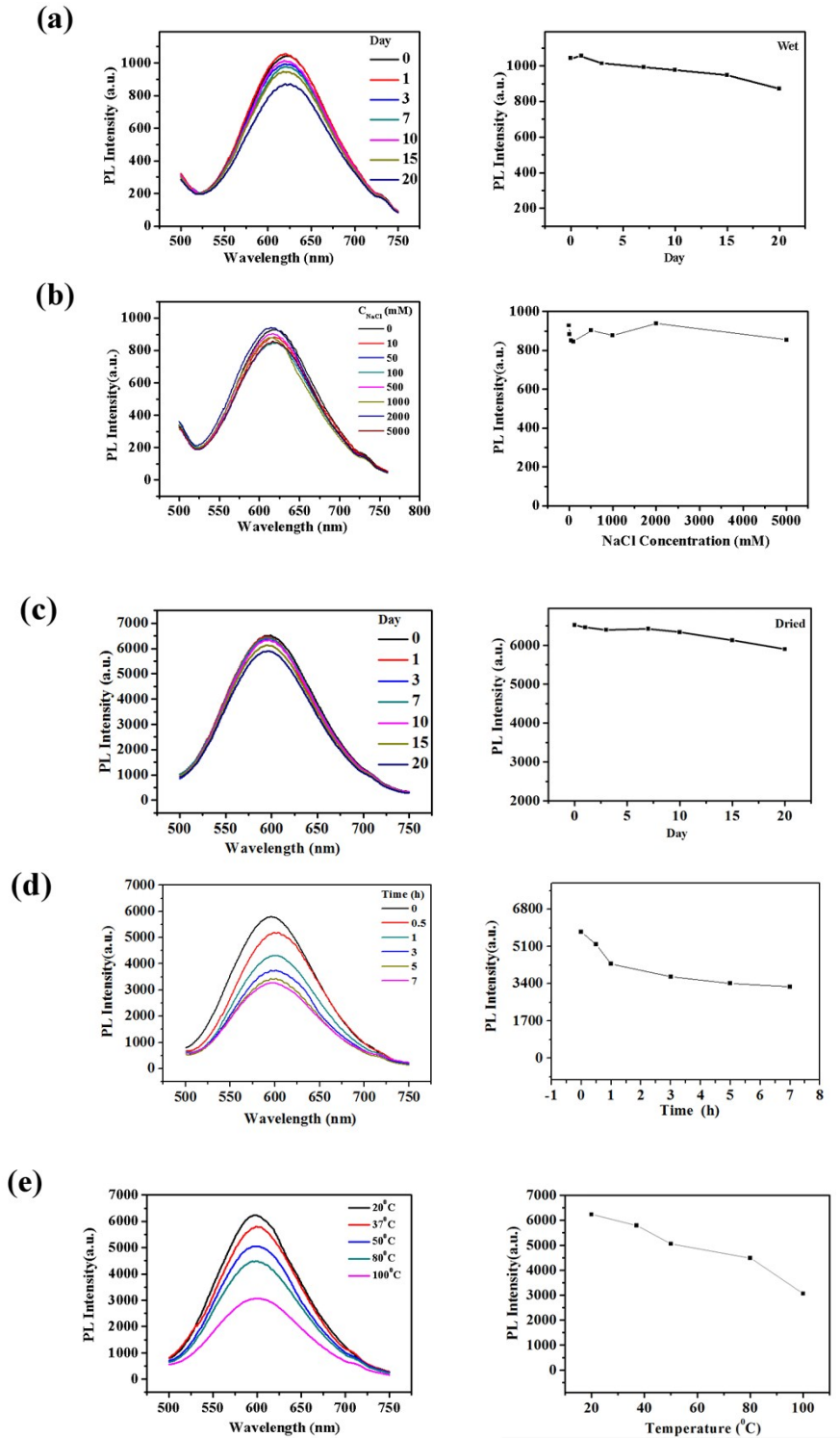
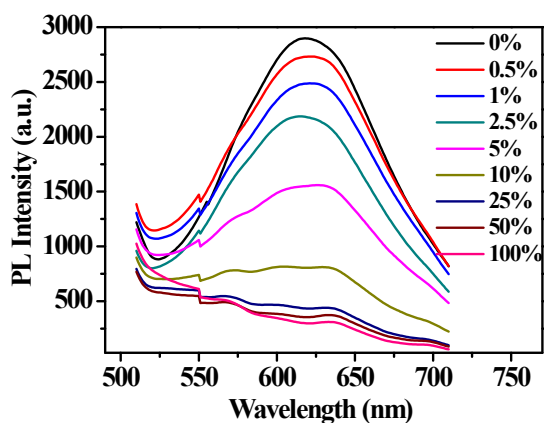
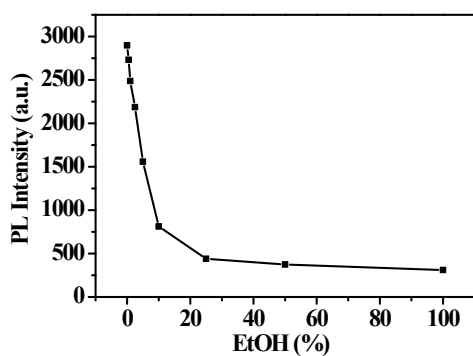


Fig. S15. The emission spectra of wet (a) and dried (c) Cu NCs/ESM at different storage time. (b) The emission spectra of Cu NCs/ESM incubated in different NaCl solutions. The emission spectra of Cu NCs/ESM exposed to 365 nm UV irradiation for different time (d) and under different temperatures (e) excited at 360 nm.

(a)



(b)



(c)

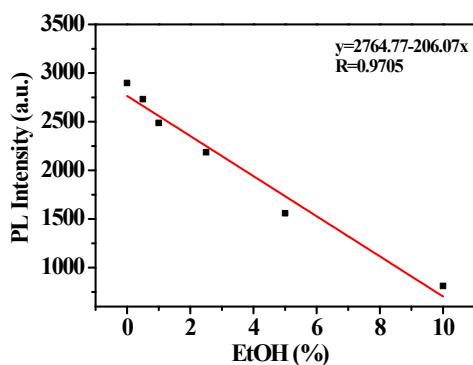


Fig. S16. (a) The series of PL emission spectra of Cu NCs/ESM exposed to ethanol solutions with different volume fractions, from 0 to 100% excited at 360 nm. (a) The plot of PL intensity versus the volume fractions of ethanol. (C) The fitted linear relationship between the PL intensity and the volume fractions of ethanol.

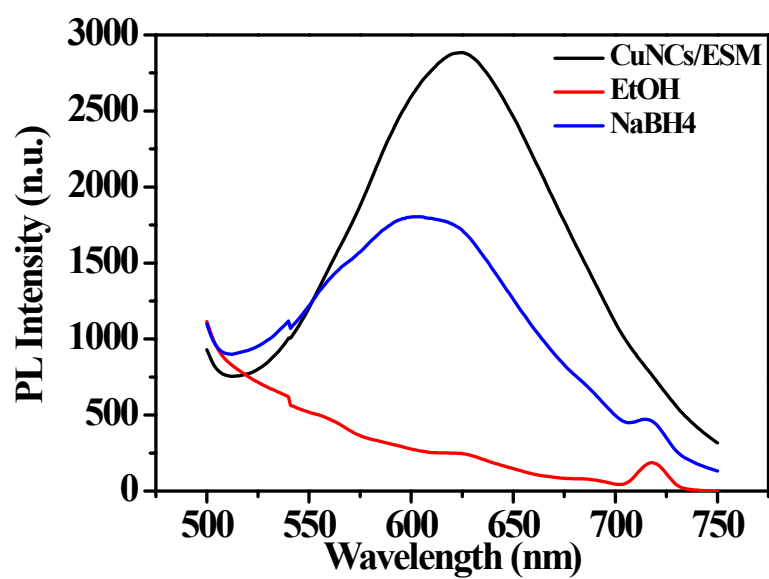
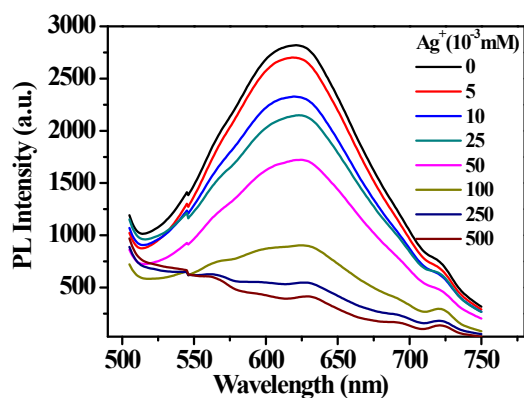
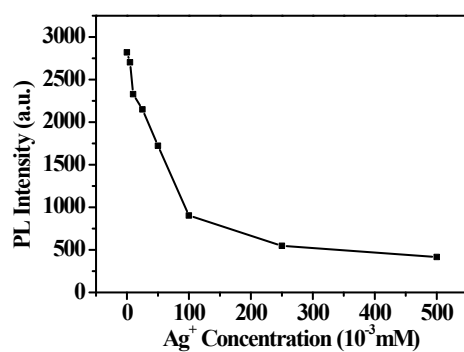


Fig. S17. The PL emission spectra of luminescent Cu NCs/ESM (black line), ethanol quenched Cu NCs/ESM (red line) and regenerated luminescent Cu NCs/ESM by NaBH₄ treatment (blue line) excited at 360 nm, respectively.

(a)



(b)



(c)

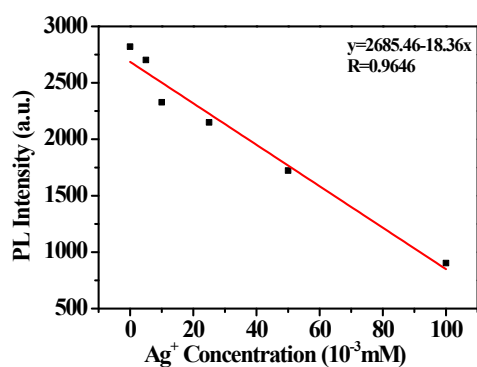
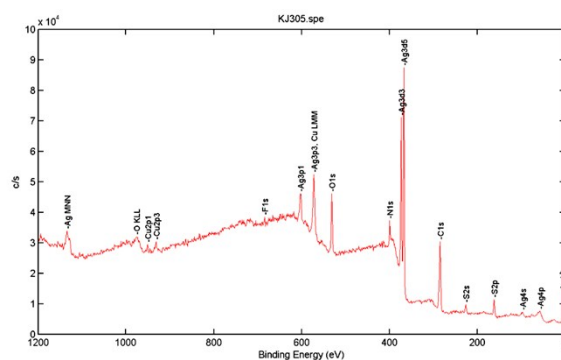
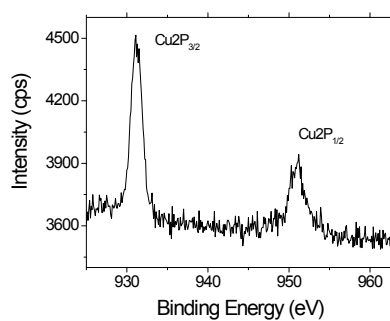


Fig. S18. (a) The series of PL emission spectra of Cu NCs/ESM in the presence of Ag⁺ ions with different concentrations excited at 360 nm. (a) The plot of PL intensity versus the concentrations of Ag⁺ ions. (C) The fitted linear relationship between the PL intensity and the concentrations of Ag⁺ ions.

(a)



(b)



(c)

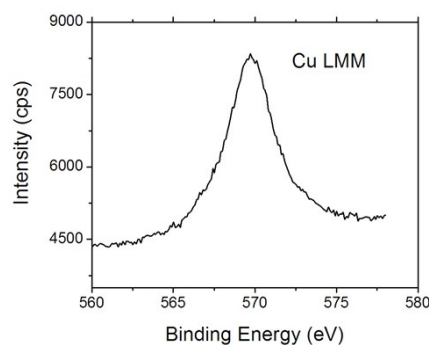
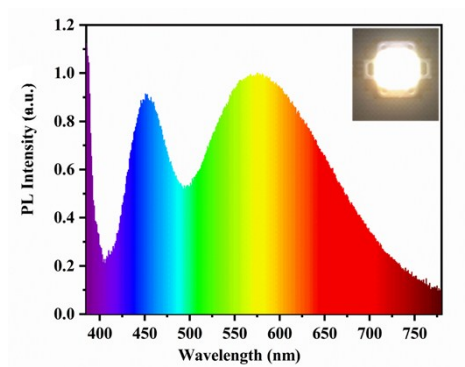
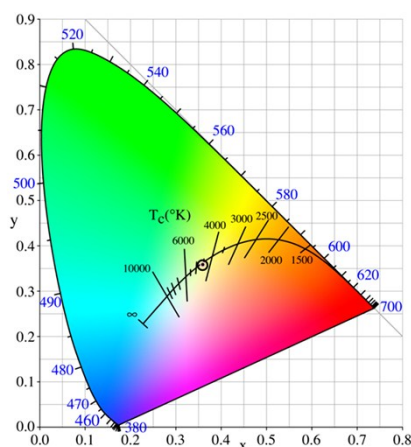


Fig. S19. (a) The XPS survey spectrum of Cu NCs/ESM composite quenched by Ag^+ ions, indicating all the expected elements, including C, O, N, S, Cu and Ag. (b) XPS spectrum of Cu 2p of Cu NCs/ESM quenched by Ag^+ ions. The two peaks at 931.13 and 951.23 eV were assigned to the Cu $2\text{P}_{3/2}$ and Cu $2\text{P}_{1/2}$ of Cu(0)/Cu(I) states well. The absence of satellite peak at around 942 eV also suggested the absence of Cu(II) in the Cu NCs/ESM composite quenched by Ag^+ ions. (c) The Auger electron spectrum (AES) in the Cu LMM region of Cu NCs/ESM quenched by Ag^+ ions. The peak at 569.7 eV further confirmed the presence of Cu(I) component in the composite.

(a)



(b)



(c)

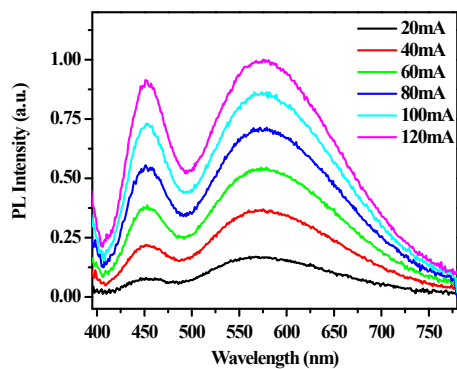


Fig. S20. (a) Emission spectra of the fabricated WLED employing the orange emitting Cu NCs/ESM composite and commercial blue emitting $\text{BaMgAl}_{10}\text{O}_{17}:\text{Eu}$ as the color converters. Inset shows a luminescence image of the operating device. (b) The chromaticity diagram of the WLED. (c) The PL spectra of the WLED under different driven currents from 20 to 120 mA.

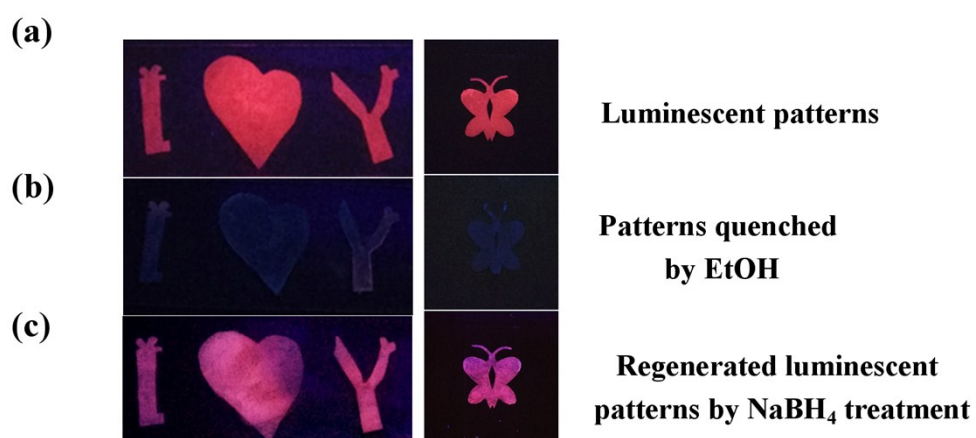


Fig. S21. The advanced surface luminescent patterning based on the developed 2D Cu NCs/ESM composite fabrication strategy. (a) The as-fabricated luminescent patterns. (b) The non-luminescent patterns quenched by EtOH. (c) The regenerated luminescent patterns by NaBH₄ treatment under 365 nm UV light.